

PHYSICS CONTRIBUTION

INTERNAL TARGET VOLUME DETERMINED WITH EXPANSION MARGINS BEYOND COMPOSITE GROSS TUMOR VOLUME IN THREE-DIMENSIONAL CONFORMAL RADIOTHERAPY FOR LUNG CANCER

HELEN A. SHIH, M.D., M.S., STEVE B. JIANG, PH.D., KHALED M. ALJARRAH, M.S.,
KAREN P. DOPPKE, M.S., AND NOAH C. CHOI, M.D.

Department of Radiation Oncology, Massachusetts General Hospital and Harvard Medical School, Boston, MA

Purpose: Gross tumor volume (GTV) of lung cancer defined by fast helical CT scan represents an image of moving tumor captured at a point in active respiratory movement. However, the method for defining internal margins beyond GTV to account for its expected physiologic movement and all variations in size and shape during the administration of radiation has not been established. The goal of this study was to determine the internal margins with expansion margins beyond individual GTVs defined with (1) fast scan at shallow free breathing, (2) breath-hold scans at the end of tidal volume inspiration and expiration, and (3) 4-s slow scan to approximate the composite GTV of all scans.

Methods and Materials: A series of sequential CT scans were acquired with (1) a fast helical scan at shallow free breathing and (2) breath-hold scans at the end of tidal volume expiration and inspiration for the first 6 patients, and (3) a 4-s slow scan at quiet free breathing, which was added for the latter 7 patients. We fused breath-hold scans and the 4-s slow scan to the fast scan at shallow free breathing to generate the composite GTV. Margins necessary to encompass the composite GTV beyond individual GTVs defined by either fast scan at quiet free breathing, breath-hold scans, or the 4-s slow scan at quiet free breathing were defined as expansion or internal margins and termed the *internal target volumes*. The centroid of the tumor volume was also used as another reference for tumor movement.

Results: Thirteen patients with 14 tumors were enrolled into the study. Substantial tumor movement was noted by either the extent of internal margins beyond each GTV or the movement of the centroid. Internal margins varied significantly according to the method of CT scanning for determination of GTV. Even for tumors in the same lobe of the lung, a wide range of internal margins and significant variation in the centroid movement in all directions (*x*, *y*, and *z*) were observed. The GTV of a single fast helical scan at free breathing (*n* = 14) required the largest internal margin (mean, 3.5 mm; maximum, 18 mm; standard deviation [SD], 4.2 mm) to match the composite GTV, compared with those of the 4-s slow scan (mean 2.7 mm, maximum 14 mm, SD 3.5 mm) or combined breath-hold scans (mean 1.1 mm, maximum 9 mm, SD 1.9 mm). Internal margins (expansion margins) required to approximate the composite GTV in 95% of cases were 13 mm, 10 mm, and 5 mm for the GTVs of a single fast scan, 4-s slow scan, and breath-hold scans at the end of tidal volume inspiration and expiration, respectively.

Conclusions: The internal margins required to account for the internal tumor motion in three-dimensional conformal radiotherapy are substantial. For the use of symmetric and population-based margins to account for internal tumor motion, GTV defined with breath-hold scans at the end of tidal volume inspiration and expiration has a narrower range of internal margins in all directions than that of either a single fast scan or 4-s slow scan.
© 2004 Elsevier Inc.

: Lung cancer, Tumor movement associated with respiration, Internal target volume, Gross tumor volume, Composite tumor volume, 3D-CRT, CT scan, Geographic miss.

INTRODUCTION

The evolution in the management of lung cancer has shown the necessity for the administration of a high radiation dose to achieve local tumor control (1–5). However, radiation

therapy with a two-dimensional treatment plan is limited in its ability to spare surrounding normal tissues while administering a high dose to target tissues. The introduction of three-dimensional conformal radiotherapy (3D-CRT) planning has significantly facilitated the definition of both target

Reprint requests to: Noah C. Choi, M.D., Massachusetts General Hospital, Department of Radiation Oncology, 100 Blossom Street, Boston, MA 02114. Tel: (617) 726-6050; Fax: (617) 726-3606; E-mail: nchoi@partners.org

Presented at the Annual Meeting of the American Society for Therapeutic Radiology and Oncology, October 5–8, 2002, New

Orleans, LA.

This work was supported in part by National Institutes of Health grant EB00290.

Received Jan 9, 2004, and in revised form May 3, 2004. Accepted for publication May 10, 2004.

tissue and normal organs. This has enabled quantitative assessment of dose delivery to all defined structures, both target and normal tissues, with dose–volume histograms. However, it has become increasingly apparent that treatment planning based on standard fast CT scanning of the chest alone is often inadequate. Fast helical CT scanners have become widely used. These scanners typically acquire images at <1 s per rotation. Each image slice within a CT scan defines the thoracic anatomy at only one point in time of respiratory movement and one short range (1.0–2.0 cm) of the thorax. Thus, incongruity can be seen between image slices within one CT scan series as a result of data acquisition over time.

Ross *et al.* (6) reported significant movement of intrathoracic neoplasms, using ultrafast CT. Twenty patients with intrathoracic neoplasms were evaluated with ultrafast (cine) CT to determine the contribution of tumor motion to geographic errors. The treatment portals were set up with conventional simulation techniques and then scanned with cine CT. Eight tomographic levels were studied, with 10 images per level over 7 s. Major geographic misses were detected in 3 patients (15%) and minor geographic misses in an additional 3 (15%). Five of six hilar lesions showed significant lateral motion (average = 9.2 mm) with cardiac contraction, and three of four lower lobe lesions showed significant craniocaudal movement with respiration. Mediastinal lesions moved an average of 8.7 mm laterally. Lesions in the upper lobes showed minimal movement (average = 2.2 mm), and tumors attached to the chest wall showed no measurable movement. Stevens *et al.* (7) measured respiration-driven lung tumor motion during routine simulation by having double-exposed anteroposterior (AP) and lateral radiographs at the maximal inspiration and expiration. The superior–inferior (SI) tumor dimension was measured on the double-exposed radiograph at the maximal inspiration and expiration and compared with the SI tumor dimension measured on an AP simulation radiograph taken during quiet respiration. Both radiographs were obtained during the same simulation procedure, with the same isocenter, with the patient in the treatment position. The tumor motion was determined by subtracting the apparent tumor size on the free-breathing simulation film from the tumor size on the double-exposure radiograph. Seven of 11 central tumors demonstrated some motion, compared with 5 of 11 peripheral tumors. Four of 5 upper lobe tumors moved, compared with 8 of 17 tumors in either middle or lower lobes. The mean (\pm SD) motion of the fourth rib was 7.3 ± 3.2 mm (range, 2–15 mm). Pulmonary functional parameters included forced expiratory volume in 1 s of 1.8 ± 1.2 liters (range, 0.55–5.33 L), diffusing capacity of 14.0 ± 6.5 ml/min/mm Hg (range, 7.8–21.9), and total lung capacity of 6.5 ± 1.2 L (range, 3.3–8.4 L). None of these parameters correlated with tumor motion. Tumor motion was not predictable by tumor size, location, or pulmonary function.

Shimizu *et al.* (8) conducted a study in which 16 lung tumors were scanned sequentially at the same table position. The location for repeat imaging was determined by the

image slice that best depicted the tumor on an initial free-breathing CT scan. Twenty sequential images were taken at one image per second at 2-s intervals during normal free breathing. Surprisingly, tumor was not visible on 21% (75 of 357) of the images. The incidence of disappearance of the tumor from the images was as follows: lower lobe tumor 39.4% (71 of 180), middle lobe tumor 8.9% (4 of 45), and upper lobe tumor 0 (0 of 89), $p < 0.01$. Shimizu *et al.* also measured the AP displacement of the tumor in each image to determine the proportion of tumors that would be missed by a lateral radiation treatment field designed from the baseline free-breathing scan. There was a mean displacement of 6.42 mm (range, 2.1–24.4 mm) between the surface of the CT table and the posterior border of the tumor. These data indicate that 3D planning based solely on fast CT scans at free breathing carries a significant risk for suboptimal treatment. Balter *et al.* (9) compared fast CT scan at free breathing with breath-hold scans at the end of tidal volume inspiration and expiration for the movement of the thoracic and abdomen organs. The variation in the path-length of radiation beam was an average of 5 mm but ranged to as much as 25 mm. Again, these changes might significantly alter dosimetry by unintentional miscalculation of tissue separation and tumor depth, thus causing underdosing of tumor or increased toxicity to surrounding normal tissues.

The International Commission on Radiation Units and Measurements (ICRU) recommends that planning target volume (PTV) include margins beyond the clinical target volume (CTV) or gross tumor volume (GTV) (if CTV = GTV) to account for internal organ motion and setup error (10). To distinguish the need for and magnitude of expansion margins that are necessary beyond CTV or GTV (if CTV = GTV) to account for GTV movement associated with physiologic internal organ motion from that for setup error, ICRU introduced the term *internal margin* to account for expected physiologic movement and variations in geometry of the CTV or GTV (if CTV = GTV) during the administration of radiation therapy. The term *internal target volume* (ITV) was also introduced by the ICRU to specify a target volume that includes CTV or GTV (if CTV = GTV) and its internal margin.

The purpose of the study reported here was to better define internal margins and ITV. The study plan consisted of the following: (1) GTVs from breath-hold scans at the end of tidal volume inspiration and expiration and a 4-s slow scan were fused to that of a single fast helical scan to determine composite GTV in each tumor, and it was assumed to represent ITV; (2) internal margins of individual GTVs were determined with expansion margins that are required to approximate the composite GTV in x , y , and z axes; and (3) patterns of tumor movement relative to the tumor location in the lung were evaluated according to the movement of the tumor centroid, defined as the center of contoured tumor volume, independent of tumor density.

METHODS AND MATERIALS

Patients

Eligibility criteria included (1) histologic or cytologic evidence of non-small-cell or small-cell carcinoma of the lung, (2) medically inoperable Stage I and II disease and Stage III disease defined by T1–2, N0–3, M0 lesions according to the staging of the American Joint Committee on Cancer, (3) a performance score of 0–2 by the Eastern Cooperative Oncology Group scale, (4) candidacy for definitive radiation therapy, and (5) ability to follow instructions and perform voluntary breath-holds at the end of tidal volume inspiration and expiration. Patients who did not meet these criteria were ineligible.

Instructions for quiet free breathing and expiratory and inspiratory breath-holds were reviewed by a physician. Quiet free breathing, both for fast scans and 4-s slow scans, was defined as normal, unlabored breathing devoid of sighing, yawning, gasping, or deep inspiratory or expiratory efforts. For breath-hold scans, patients were instructed to hold their breath at the end of normal inspiration or expiration (end tidal volume), just before they would normally change from inhaling to exhaling or vice versa. The breath-hold technique was practiced before scanning, and the length of breath-hold was approximately 10 s. All patients understood instructions for breathing patterns and were willing participants in the study before proceeding with the scans. All scans were performed on the basis of patient compliance without spirometry. Monitoring of patient behavior during scan acquisition was consistent with patient compliance.

CT scans

The CT scanner used for all data acquisition was a GE LightSpeed QX/i (GE Medical Systems, Milwaukee, WI). Patients were positioned supine and immobilized with a standard wingboard, with their arms above their head. The initial 6 patients had a series of three CT scans. These were obtained with high-quality fast helical acquisition of 0.8 s per image. The scans were taken (1) at quiet free breathing at tidal volume, (2) at breath-hold at the end of the tidal volume inspiration, and (3) at breath-hold at the end of the tidal volume expiration. All patients were compliant and were carefully instructed to breathe quietly throughout the initial free-breathing scan. The fast scan at free breathing, acquired at four slices every 0.8 s, typically contained 100 images at 3.75-mm thickness and served as the template for treatment planning. For the subsequent scans, patients held their breath at the end of tidal volume inspiration and expiration sequentially. Because of the time limitation in maintaining the breath-hold positions, these images were limited in number to the 20–30 slices spanning the region of the tumor as defined on the fast CT scan at free breathing. Patients held their breath typically for 10 s per breath-hold position. For the latter 7 patients, a slow CT scan with a 4-s-per-revolution image acquisition at tidal volume free breathing was added to image the tumor with 3–4-cm

cranial and caudal margins. Because the time for an average respiratory cycle is approximately 4 s (11), we hypothesized that a 4-s acquisition per image would detect the range of tumor motion and shape throughout the normal respiratory cycle. For all CT scans, a pitch of 3 was used with a standard reconstruction algorithm using 360° data acquisition. Four slices per rotation of 3.75-mm thickness resulted in 15-mm intervals.

Once data were acquired, the three scans limited to the region of tumor (breath-hold scans at the end of tidal volume inspiration and expiration and 4-s slow scan at tidal volume free breathing) were transferred to a commercial treatment planning system (Focus; Computerized Medical System, St. Louis, MO) and fused to the standard fast scan obtained in free breathing with commercially available software (Focal Fusion; Computerized Medical Systems). Fusions were rigid body. The vertebral spine was used as the reference for alignment between all scans because this was judged to be the anatomic structure least affected by normal cardiac and respiratory motion. Slight differences in thoracic cavity contour were noted between fused scans, but bony anatomy was relatively well aligned along the posterior aspect of the ribs and the spine, such that minor changes at the anterior aspect of the thorax were assumed to be due to the types of breathing in the study. Tumor volume was subsequently drawn on each of the multiple scans for each patient. All image fusions and definitions of tumor contour were performed by a single physician (H.A.S.) and reviewed by a second radiation oncologist with thoracic expertise (N.C.C.).

Data analyses

All CT data, along with the contours, were subsequently analyzed with software developed in house. The software is written in Interactive Data Language (Research Systems, Boulder, CO). It reads CT data and contours for all scans (free-breathing scan, slow scan, and breath-hold scans) and for each GTV, calculates the volume, mass, average density, center of mass, centroid, and center of bounding box, as well as the change of margins in three principal directions. The centroid of the GTV, which is independent of tumor density, was used to assess the extent of tumor movement by means of the magnitude of its displacement in all three directions: right–left (x axis), SI (y axis), and AP (z axis). The centroid of the GTV defined by the fast helical scan was set as the reference, and the amount of displacement was measured according to the distance between the centroids of the reference and test GTVs.

The ITV was defined as the sum of the individual GTVs defined at different phases of respiration and the volume that it travels under normal respiratory and cardiac movement. It was hypothesized that the best estimate of the ITV is the composite volume of each GTV from all three scans. This was also termed *composite GTV*. The composite GTV (ITV) should be inclusive of individual GTVs from all available planning CT scans. The internal margin is the

Table 1. Patient characteristics

Patient no.	Tumor no.	Age (y)	Location	T stage	Size (cm)	4-s slow scan
1A	1	70	LUL	T2	4.5 × 4.0	N
1B	2	70	RUL	T1	2.3 × 1.3	N
2	3	90	RUL	T1	5.7 × 3.9	N
3	4	76	LUL	T1	1.8 × 1.7	N
4	5	69	LLL	T3	6.0 × 3.5	N
5	6	66	RML	T1	1.9 × 1.5	N
6	7	79	LUL	T3	3.0 × 4.0	N
7	8	73	LUL	T2	4.5 × 3.0	Y
8	9	65	LUL	T2-3	2.0 × 1.2	Y
9	10	73	LLL	T3	4.0 × 4.0	Y
10	11	73	LMSB	T3	2.0 × 1.3	Y
11	12	67	RLL	T2	3.7 × 3.0	Y
12	13	68	RLL	T2	3.8 × 4.2	Y
13	14	77	LUL	T1	1.6 × 1.1	Y

Abbreviations: LUL = left upper lobe; LLL = left lower lobe; LMSB = left main stem bronchus; RUL = right upper lobe; RML = right middle lobe; RLL = right lower lobe; T = tumor; N = no; Y = yes.

expansion margin beyond each GTV to approximate the composite GTV.

To determine the internal margin for the individual GTV of each scan defined by (1) fast helical scan at quiet free breathing, (2) breath-hold scans at the end of tidal volume inspiration and expiration, and (3) 4-s slow scan at free breathing, a bounding box was calculated and used to estimate the necessary margins to approximate the composite GTV along the three orthogonal axes (*x*, *y*, and *z*). Thus, for the first seven tumors, the composite GTV was determined by the fusion of the fast scan at quiet free breathing and both breath-hold scans. For the remaining seven tumors, the composite GTV was defined by the fusion of the 4-s slow scan at free breathing to that of the fast scan at free breathing and the combined GTV of both breath-hold scans at the end of tidal volume inspiration and expiration. For the purpose of this study, no additional margin was added to the GTV to define either CTV or PTV.

RESULTS

Patient characteristics

A total of 13 patients with 14 tumors participated in this study. All patients had lung cancer and were simulated for 3D-CRT between February 2001 and April 2002. One patient had two separate primary lesions, one at the lingular lobe of the left upper lobe and the other at the right upper lobe (Patients 1A and 1B of Table 1). Tumor size, measured as the maximal dimension on any orthogonal plane but most commonly on axial image, ranged from 1.6 × 1.1 cm to 6 × 3.5 cm. The patient characteristics and their tumor size and location are listed in Table 1.

Patterns of tumor motion as determined with tumor centroid

The centroid of each tumor was determined as the center of tumor volume drawn by the physician. We postulated that the centroids of the gross tumors determined with fast scan

at free breathing and with 4-s slow scan would lie between the centroids of those defined with the breath-hold scans at the end of tidal volume inspiration and expiration. Contrary to expectations, the motion of the centroid for each tumor was markedly variable as referenced by the standard fast scan at quiet free breathing in all three planes of SI (cranial-caudal), left-right, and AP directions (Figs. 1a-1c). There was no reproducible pattern of centroid position in any axis.

Patient 1 had two tumors with different histologic types: one (Tumor 1) at the left upper lobe and the other (Tumor 2) at the right upper lobe of the lung (Table 1). The magnitude of tumor motion between these two tumors was quite different in all directions (*x*, *y*, and *z*) (Figs. 1a-1c). Even for the tumors in the same lobe, no consistent pattern of tumor movement was found. Six of 14 tumors (Tumors 1, 4, 7, 8, 9, and 14) were located at the left upper lobe of the lung. The extent of tumor motions at *x*, *y*, *z* directions were markedly variable among the tumors without consistent patterns (Figs. 1a-1c). There were four lower lobe tumors, two on each side. The extent of the centroid displacement at *x*, *y*, and *z* directions was again markedly variable among these (Figs. 1a-1c).

In several patients, the centroids of breath-hold scans at the end of tidal volume inspiration and expiration were closer to each other than to that of the fast scan at quiet free breathing. In addition, no correlation was noted between the centroid of tumor determined with 4-s slow scans and that of the breath-hold scans. When the centroids of the fast and 4-s slow scan at free breathing were compared, there was no consistent and reproducible pattern. These data were combined to plot the net displacement of the centroids in SI, AP, and lateral directions (Fig. 1d).

Internal margins (expansion margins) of GTV to approximate composite GTV

Internal margins for the GTV of a single fast helical scan at free breathing (*n* = 14) consisted of a mean 3.5 mm, maximum 18 mm, and standard deviation (SD) 4.2 mm,

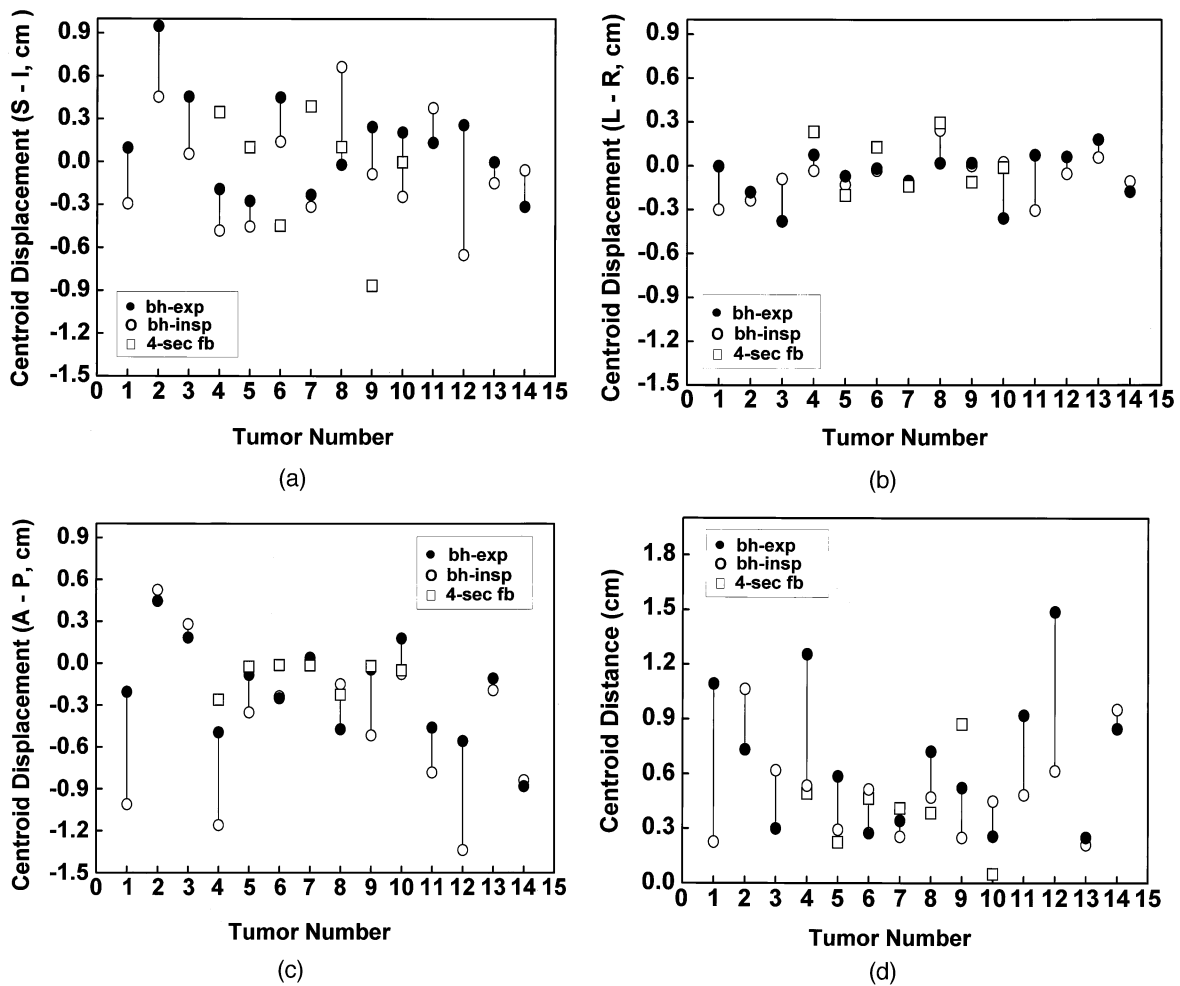


Fig. 1. Extent of tumor motion in the (a) superior–inferior (S-I), (b) left–right (L-R), and (c) anterior–posterior (A-P) directions, and (d) net tumor motion were determined by the movement of tumor centroid (defined as the center of contoured tumor volume, independent of tumor density) and related to that of a fast scan at quiet free breathing. Filled circles represent breath-hold at the end of tidal volume expiration (bh-exp); open circles represent breath-hold at the end of tidal volume inspiration (bh-insp); open squares represent 4-s slow scanning at quiet free breathing (4-sec fb). Tumor numbers 1 and 2 are from the same patient.

compared with mean 2.7 mm, maximum 14 mm, and SD 3.5 mm for the GTV of 4-s slow scan and mean 1.1 mm, maximum 9 mm, and SD 1.9 mm for the combined GTV of breath-hold scans at the end of tidal volume inspiration and expiration (Table 2). The GTV determined with fast helical scan at free breathing showed the largest variation in internal margins, with a maximum displacement of 17.8 mm in the posterior direction, whereas the GTV of breath-hold scans showed the narrowest internal margins, with a range from 0.4 mm (posterior direction) to 2.2 mm (anterior direction). Although the GTV defined by the 4-s slow scan was larger than that of the fast scan at free breathing, it was not as close as the combined GTV of breath-hold scans in matching with the composite GTV.

Thus, the expansion margins (internal margin) required to approximate the composite GTV in 95% of cases were 13 mm (mean \pm 2 SD), 10 mm, and 5 mm for the GTVs of a single fast scan, 4-s slow scan, and combined GTV of

breath-hold scans at the end of tidal volume inspiration and expiration, respectively.

DISCUSSION

The method of determining the internal margin, representing the expansion margin beyond CTV or GTV (if CTV = GTV), to account for the movement and deformation of GTV associated with physiologic organ motion has not been standardized. Thus, how much internal margin one should add to GTV, which is defined by a fast helical scan to avoid geographic miss, has been largely left to clinical judgment and fluoroscopic evaluation, if necessary.

Clinical research in 3D-CRT for radiation dose escalation has been conducted with an expansion margin of 10–15 mm from CTV or GTV (if CTV = GTV) to PTV for both internal margin and setup error, with the GTV defined with a single fast scan at free breathing. If it is assumed that an

Table 2. Maximum and mean values (in millimeters) of internal margins

	Combined GTVs of bh-insp and bh-exp		4-sec-fb GTV		fs-fb GTV	
	Max	Mean	Max	Mean	Max	Mean
Left	3.6	0.5	7.7	3.2	11.4	2.3
Right	3.8	1.0	14.3	2.6	14.3	2.2
Anterior	8.9	2.2	6.4	1.4	12.0	2.7
Posterior	3.1	0.4	6.4	2.6	17.8	6.0
Superior	5.9	0.6	7.0	1.4	11.9	3.7
Inferior	8.9	1.7	8.9	5.1	11.9	3.8
Mean		1.06		2.71		3.45
SD		1.93		3.48		4.25

Abbreviations: GTV = gross tumor volume; bh-insp = breath-hold scan at the end of tidal volume inspiration; bh-exp = breath-hold scan at the end of tidal volume expiration; 4-sec-fb = 4-s slow scan at free breathing; fs-fb = fast scan at free breathing; SD = standard deviation.

Internal margins beyond the boundary of (1) combined GTV of bh-insp and bh-exp, (2) GTV of 4-sec-fb, and (3) GTV of fs-fb to approximate the composite GTV of all scans.

expansion margin of ≥ 5 mm is required for setup errors, many studies have used only a 5–10-mm expansion for internal margin to account for the movement and deformation of GTV associated with physiologic organ movement (12–15). However, based on the available clinical data, it is a reasonable assumption that these studies are at risk for increased local failure as a result of geographic miss in a certain proportion of patients. Therefore, it is an important issue in high-dose radiation therapy that PTV includes an internal margin adequate for the coverage of tumor movement and deformation associated with physiologic organ movement.

Ekberg *et al.* (16) measured the movement of GTV associated with shallow respiration and cardiac motion using fluoroscopy in 20 patients with lung cancer. The magnitudes of GTV movement with quiet breathing consisted of a mean 2.4 mm, maximum 5.0 mm, and SD 1.4 mm in the medio-lateral and dorsoventral directions, and mean 3.9 mm, maximum 12.0 mm, and SD 2.6 mm for the craniocaudal direction. They also evaluated 553 electronic portal images from the 20 patients for setup errors. Discrepancies between the planned and actual field positions were measured, and the systematic and random errors were identified. The systematic setup errors included a mean 2.9 mm, maximum 16.4 mm, and SD 3.8 mm in the transversal plane and mean 3.6 mm, maximum 15.7 mm, and SD 4.6 mm in the craniocaudal direction. The expansion margins required to cover the GTV movement plus setup errors in 95% of the observed cases were 15.7 mm for transversal (x , z) and 22 mm for craniocaudal (y) directions. On the basis of these data, the authors stated that they use a margin of 11 mm for the transversal plane and 15 mm for the craniocaudal direction in the daily clinical routine. However, these expansion margins that the authors chose to use are adequate for only 75% of patients.

We fused GTVs defined with a single fast helical CT scan, 4-s slow scan, and breath-hold scans at the end of tidal volume expiration and inspiration to determine the composite GTV, which represents GTV of each scan plus internal

margins. The internal margins were determined with the expansion margins that were required for each GTV from a single scan or combined scans to approximate the composite GTV. The internal margins for GTV defined with a fast scan at free breathing consisted of a mean 3.3 mm and maximum 17.8 mm in the transversal plane, compared with mean 3.75 mm and maximum 11.9 mm in the craniocaudal direction (Table 2). The internal margins for GTV defined with a 4-s slow scan at free breathing included a mean 2.45 mm and maximum 14.3 mm in the transversal plane, compared with mean 3.25 mm and maximum 8.9 mm in the craniocaudal direction. The internal margins derived from our study are very similar to those of Ekberg *et al.*, except that the maximum in the transversal plane was much larger than in their study.

The extent and the range of variation in the internal margins are also related to the types of planning CT scans. The internal margin for GTV defined with a single fast scan at free breathing is the largest, whereas it is the least for the GTV obtained with breath-hold scans at the end of tidal volume inspiration and expiration. It is hypothesized that the likelihood of a geographic miss increases as the standard deviation of internal margin becomes larger when a population-based margin is used to account for the movement of GTV. Our data suggest that GTV defined with breath-hold scans at the end of tidal volume inspiration and expiration offers the least risk for geographic miss, compared with either a 4-s slow scan or a single fast scan at free breathing (Table 2). It is also shown that a population-based internal margin might not serve all patients well, because there is a significant individual variation in the extent of movement and deformation of GTV associated with respiratory and cardiac function (Figs. 1a–1d). To mimic the routine clinical setting, we obtained fast helical CT scans at tidal volume free breathing, breath-hold at the end of tidal volume inspiration and expiration, and 4-s slow scan at free breathing solely based on verbal instructions and patient compliance. Thus, the absence of an adequate control of the respiratory volume or cycle with spirometry during CT scanning might

have introduced some inaccuracies. However, the fact that the ITV determined with the breath-hold scans is larger than that of the 4-s scan at free-breathing suggests that the patients' compliance to the instruction for breath-holding was reasonable.

Van Sörnsen de Koste *et al.* (17) performed six spiral CT scans (three rapid and three slow) in 7 patients with lung tumors located in the lower lobe to determine the minimal number of scans required for the determination of internal margins. Slow CT scans generated larger and more reproducible target volumes than did rapid planning scans, with a mean ratio between the overlapping and encompassing volume of $71.9 \pm 8.7\%$ and $58.0 \pm 12.7\%$, respectively. When only a single slow CT scan was used for planning, an addition of a symmetrical 3D margin of 5 mm ensured 99% coverage of the "optimal" target volume that was derived from summation of the target volumes from all six scans. The authors concluded that the PTVs derived from a single slow CT scan plus a 5-mm internal margin covered the "optimal" PTV generated from six scans and that only two CT scans (i.e., a full rapid scan of the entire thorax and a limited slow scan) are necessary for treatment planning in peripheral lung cancers.

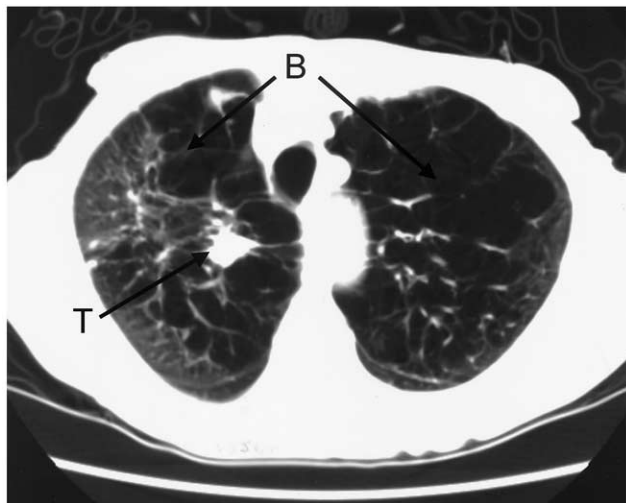
However, our results are not in agreement with the conclusions of van Sörnsen de Koste *et al.* (17). For the composite GTV, we fused GTVs of breath-hold scans at the end of tidal volume inspiration and expiration to that of a fast helical scan for a better definition of internal margins at the extreme positions in normal tidal volume breathing for the initial 6 patients with seven tumors and created similar fusions with the addition of the 4-s slow scan for the subsequent 7 patients. Because of the breath-hold scans at the end of tidal volume inspiration and expiration, the composite GTV determined in our study might have been larger than that of van Sörnsen de Koste *et al.* (17). Our data indicate that expansion margins (internal margins) required to approximate the composite GTV in 95% of cases were 13 mm, 10 mm, and 5 mm for the GTVs of a single fast scan, 4-s slow scan, and breath-hold scans at the end of tidal volume inspiration and expiration, respectively. Even with some differences in the method for determining composite GTV and tumor movement between these two studies, we observed that the extent of tumor movement at *x*, *y*, and *z* directions was markedly variable among the tumors, without consistent patterns (Figs. 1a–1c). Even for the tumors in the same lobe, no consistent pattern of tumor movement was found. Six of 14 tumors (Tumors 1, 4, 7, 8, 9, and 14) were located in the left upper lobe of the lung. The extent of the centroid displacement at *x*, *y*, and *z* directions was markedly variable among the tumors. There were four lower lobe tumors, two on each side (Tumors 5, 10, 12, 13). Marked variation in the extent of the centroid displacement at *x*, *y*, and *z* directions was again noted among these four tumors (Figs. 1a–1c).

Population-based margins for tumor movement and setup errors can be too large for at least 75% of patients if they are designed for the coverage of 95% of patients. In addition,

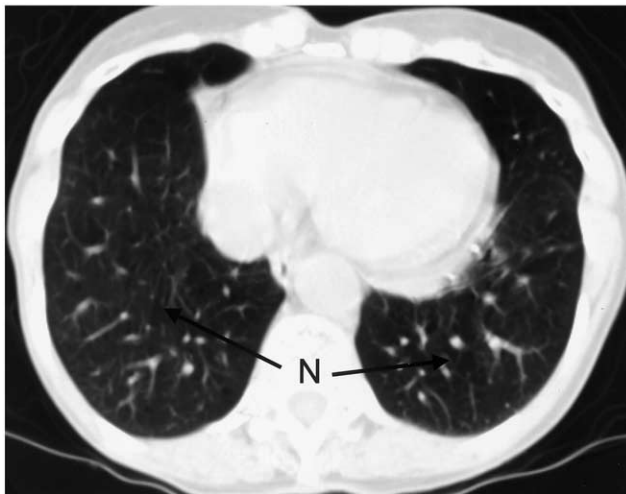
the extent of tumor movement is not uniform in all *x*, *z*, and *y* directions. Therefore, better normal tissue sparing might be achieved if the internal margins are decreased and optimized for individual patients. Indeed, clinical research in tumor tracking, respiratory gating, or breath-hold techniques is in progress in an attempt to optimize the size of internal margins (18–26). Tumor tracking is an attractive approach, which requires highly specialized technology (18, 19). Respiratory gating systems are based on reflective skin markers or airflow parameters and are being tested (20–23). Breath-hold technique at deep inspiration is another approach for sparing normal lung tissue surrounding GTV (24–26).

However, the magnitude of gain in preserving pulmonary tissue with the specialized technologies depends on clinical situations. The majority of patients with medically inoperable Stages I and II lung cancer have severe chronic obstructive pulmonary disease (COPD), and their tumor is often situated in the region of the lung with extensive bullae and very little residual function. An axial view of a CT scan in a patient with medically inoperable Stage I non-small-cell lung cancer (T1 lesion) involving the right upper lobe shows a tumor in the region with severe COPD and multiple bullae (Fig. 2a). An axial view of a CT scan at the lower chest of the same patient showed that the lower lobes of the lung are relatively well preserved from COPD (Fig. 2b). In such a situation, an improvement in overall pulmonary function was observed after radiation therapy to the region of tumor (27, 28). In locally advanced-stage lung cancer, the primary tumor might move relatively little in association with respiration when it is attached or anchored into the surrounding normal organs or tissues (T3 or T4 lesion), such as mediastinum, chest wall, or vertebrae, which moves relatively little with respiratory movement.

Four-dimensional (4D) CT might be able to define GTV with a lesser degree of deformation than fast helical CT scan in 3D-CRT planning (29, 30). Rietzel *et al.* (29) tested a 4D CT scanning protocol for quantification of respiration-induced motion and deformation of lung tumors. Instrumentation used in this study included a GE LightSpeed CT scanner (four slices, 0.8 s) and a Varian RPM respiratory monitoring system (Varian Medical Systems, Palo Alto, CA). Scans were acquired in axial cine mode, timing signals related scan acquisition with abdominal motion during respiration. Scan data were acquired at a given table position over an entire respiratory cycle. For each couch position, typically 10–15 images were reconstructed, each at a different phase of the patient's respiratory cycle. In general, as many as 1500 slices were acquired, after which the data were sorted according to small intervals of respiratory phase to generate up to 10 complete volumetric CT data sets over a respiratory period. Suitable parameters for the 4D CT scanning protocol were assessed by scanning phantoms of known size and shape placed on an oscillating sled to simulate respiratory motion. Furthermore, the accuracy of the 4D scanning data was evaluated with phantom experiments. Phantom studies showed marked improvement in the



(a)



(b)

Fig. 2. (a) Axial view of a CT scan shows a tumor (T, arrow) (T1 lesion) in a region of the right upper lobe with severe chronic obstructive pulmonary disease (COPD) and multiple bullae (B, arrows). The left upper lobe shows a similar degree of COPD. (b) Axial view of CT scan of the same patient at the lower chest shows that both lower lobes are relatively well preserved from COPD. Note normal-appearing lung parenchyma (N, arrows).

artifact with 4D CT scanning. The typical distortions of the shape and location of the objects were significantly reduced. However, artifacts in the axial slices were still present, particularly near the SI (direction of motion) aspects of the object. The volume of spheres of known size varied from -35% to $+40\%$ during the conventional helical scans. In the phantom studies, 4D scanning reduced the variation in volume of the spheres with a radius of >1.8 cm to $<7\%$. However, the utility of 4D CT scanning in 3D-CRT remains to be proven.

Gross tumor volume defined with positron emission tomography (PET) represents a time-averaged position and shape of GTV that includes tumor movement and deformation associated with respiration over a period of PET scan-

ning time for one bed position, which is usually 10–15 min. Caldwell *et al.* (31) compared fast helical CT scan with PET using a positron emitter, ^{22}Na (half-life 2.6 years, maximum positron energy 545.5 keV) at a concentration of 1 mCi/mL in a phantom study. Three fillable spheres were imaged both while stationary and during periodic motion with spiral CT and PET (20 min of image acquisition time). CT- and PET-imaged volumes were defined quantitatively according to voxel values. Ideal PTVs as internal target volume (ITV) for each scenario were calculated. CT-based PTVs were generated with margins of 7.5 mm, 10 mm, and 15 mm to account for both organ motion and setup uncertainties. PET-based PTVs were derived with an assumption that motion was captured in the PET images and only a margin (7.5 mm) for setup errors was necessary. Comparisons between CT-based and PET-based PTVs with ideal PTVs were performed.

Computed tomographic imaging of moving spheres resulted in significant distortions in the 3D image-based representations and did not, in general, result in images well representative of either moving or stationary spheres. PET images were similar to the ideal capsular shape encompassing the sphere and its motion. In all cases, CT-imaged volume was larger than that for the stationary sphere (range of excess volume, $0.4\text{--}29\text{ cm}^3$ for stationary volumes of $2.14\text{--}172\text{ cm}^3$) but smaller than that for the true motion volume. PET-imaged volumes were larger than the true motion volume (difference from ITV ranged from 3 cm^3 to 94 cm^3 for motion volumes of $1.2\text{--}243\text{ cm}^3$) and much larger than the stationary volume. With CT data, geographic miss of some part of the ideal PTV occurred for 0 of 24 cases, 11 of 24 cases, and 18 of 24 cases with a 15-mm, 10-mm, and 7.5-mm internal margin, respectively. Geographic miss did not occur in any case for the PET-based PTV. The amount of “normal tissue” included in CT-based PTVs was dramatically greater than that included in PET-based PTVs. The authors concluded that fast CT imaging of a moving tumor could result in a poor representation of the time-averaged position and shape of the tumor. PET imaging can provide a more accurate representation of the 3D volume encompassing motion of model tumors and has the potential for providing patient-specific and individualized internal target volume.

Although the phantom study by Caldwell *et al.* (31) showed that the time-averaged GTV obtained with PET imaging was very close to the ideal PTV, which is ITV, it was obtained by choosing an arbitrary threshold value of 15% relative to the maximum value within the object to match the ITV. There is a wide range of fluorodeoxyglucose (FDG) uptake in lung cancer, and one threshold value of FDG uptake would not be suitable for all patients. In addition, poor resolution of PET imaging (6–8 mm) makes the definition of the boundary of ITV less precise. Nonetheless, PET imaging can provide biochemical or molecular characteristics of tumor engraved in GTV for which radiation therapy can be tailored for the best possible outcome (32).

In our follow-up study, ITV derived from breath-hold scans at the end of tidal volume expiration and inspiration will be compared with those of 4D CT scanning and PET-based study in an attempt to improve the accuracy and definition of internal margins and internal target volume.

CONCLUSIONS

A significant degree of tumor motion occurs in association with respiratory and cardiac movement. The internal margins required to account for the internal tumor motion in 3D-CRT are substantial. Given the wide range of internal

margins at different directions (x , y , z) even for tumors in the same lobe of the lung, the use of an individualized internal margin for each patient would be desired to avoid geographic miss and spare the adjacent normal tissue. For the use of symmetric and population-based margins to account for internal tumor motion, GTV defined with breath-hold scans at the end of tidal volume inspiration and expiration has a narrower range of internal margins in all directions than that of either a single fast scan or 4-s scan. Breath-hold scanning might be a relatively simple method for improving the definition of internal target volume and tumor targeting.

REFERENCES

- Perez CA, Stanley K, Rubin P, *et al.* A prospective randomized study of various radiation doses and fractionation schedules in the treatment of inoperable non-small-cell carcinoma of the lung. Preliminary report by the Radiation Therapy Oncology Group. *Cancer* 1980;45:2744–2753.
- Choi NC, Doucette JA. Improved survival of patients with unresectable non-small-cell bronchogenic carcinoma by an innovated high-dose en-bloc radiotherapeutic approach. *Cancer* 1981;48:101–109.
- Cox JD, Azarnia N, Byhardt RW, *et al.* A randomized phase I/II trial of hyperfractionated radiation therapy with total doses of 60.0 Gy to 79.2 Gy: Possible survival benefit with greater than or equal to 69.6 Gy in favorable patients with Radiation Oncology Group stage III non-small cell lung carcinoma: Report of Radiation Therapy Oncology Group 83-11. *J Clin Oncol* 1990;8:1543–1555.
- Martel MK, Ten Haken RK, Hazuka MB. Estimation of tumour control probability model parameters from 3-D dose distributions of non-small cell lung cancer patients. *Lung Cancer* 1999;24:31–37.
- Rosenman JG, Halle JS, Socinski MA. High-dose conformal radiotherapy for treatment of stage IIIA/IIIB non-small-cell lung cancer: Technical issues and results of a phase I/II trial. *Int J Radiat Oncol Biol Phys* 2002;54:348–356.
- Ross CS, Hussey DH, Pennington EC, *et al.* Analysis of movement of intrathoracic neoplasms using ultrafast computerized tomography. *Int J Radiat Oncol Biol Phys* 1990;18:671–677.
- Stevens CW, Munden RF, Forster KM, *et al.* Respiratory-driven lung tumor motion is independent of tumor size, tumor location, and pulmonary function. *Int J Radiat Oncol Biol Phys* 2001;51:62–68.
- Shimizu S, Shirato H, Kagei K, *et al.* Impact of respiratory movement on the computed tomographic images of small lung tumors in three-dimensional (3D) radiotherapy. *Int J Radiat Oncol Biol Phys* 2000;46:1127–1133.
- Balter JM, Haken RKT, Lawrence TS, *et al.* Uncertainties in CT-based radiation therapy treatment planning associated with patient breathing. *Int J Radiat Oncol Biol Phys* 1996;36:167–174.
- International Commission on Radiation Units and Measurements. Prescribing, recording, and reporting photon beam therapy. Supplement to report 50. Report 62. Washington, DC: ICRU; 1999.
- Ganong WF. Review of medical physiology. 21st ed. New York: Lange Medical Books/McGraw-Hill, Medical Publishing Division; 2003.
- Graham MV, Purdy JA, Emami B, *et al.* Clinical dose-volume histogram analysis for pneumonitis after 3D treatment for non-small cell lung cancer (NSCLC). *Int J Radiat Oncol Biol Phys* 1999;45:323–329.
- Sim S, Rosenzweig KE, Schindelheim R, *et al.* Induction chemotherapy plus three-dimensional conformal radiation therapy in the definitive treatment of locally advanced non-small-cell lung cancer. *Int J Radiat Oncol Biol Phys* 2001;51:660–665.
- Hayman JA, Martel MK, Ten Haken RK, *et al.* Dose escalation in non-small cell lung cancer using three-dimensional conformal radiation therapy: Update of a phase I trial. *J Clin Oncol* 2001;19:127–136.
- Bradley JD, Graham MV, Winter KW, *et al.* Acute and late toxicity results of RTOG 9311: A dose escalation study using 3D conformal radiation therapy in patients with inoperable non-small cell lung cancer [Abstract]. *Int J Radiat Oncol Biol Phys* 2003;57(Suppl. 1):s137–s138.
- Ekberg L, Holmberg O, Wittgren L, *et al.* What margins should be added to the clinical target volume in radiotherapy treatment planning for lung cancer? *Radiother Oncol* 1998;48:71–77.
- van Sörnsen de Koste JR, Lagerwaard FJ, de Boer HCJ, *et al.* Are multiple CT scans required for planning curative radiotherapy in lung tumors of the lower lobe? *Int J Radiat Oncol Biol Phys* 2003;55:1394–1399.
- Kini VR, Keall PJ, Vedam SS, *et al.* Preliminary results from a study of a respiratory motion tracking system: Underestimation of target volume with conventional CT simulation [Abstract] *Int J Radiat Oncol Biol Phys* 2000;48:164.
- Shimizu S, Shirato H, Ogura S, *et al.* Detection of lung tumor movement in real-time tumor-tracking radiotherapy. *Int J Radiat Oncol Biol Phys* 2001;51:304–310.
- Kubo HD, Hill BC. Respiration gated radiotherapy treatment: A technical study. *Phys Med Biol* 1996;41:83–91.
- Ramsey CF, Scaperth D, Arwood D. Clinical experience with a commercial respiratory gating system [Abstract]. *Int J Radiat Oncol Biol Phys* 2000;48:164–165.
- Wong JW, Sharpe MB, Jaffray DA, *et al.* The use of active breathing control (ABC) to reduce margin for breathing motion. *Int J Radiat Oncol Biol Phys* 1999;44:911–919.
- Kim DJ, Murray BR, Halperin R, *et al.* Held-breath self-gating technique for radiotherapy of non-small-cell lung cancer: A feasibility study. *Int J Radiat Oncol Biol Phys* 2001;49:43–49.
- Hanly J, Debois MM, Mah D, *et al.* Deep inspiration breath-hold technique for lung tumors: The potential value of target immobilization and reduced lung density in dose escalation. *Int J Radiat Oncol Biol Phys* 1999;45:603–611.
- Sixel KE, Aznar MC, Ung YC. Deep inspiration breath hold to reduce irradiated heart volume in breast cancer patients. *Int J Radiat Oncol Biol Phys* 2001;49:199–204.
- Rosenzweig KE, Hanley J, Mah D, *et al.* The deep inspiration

- breath-hold technique in the treatment of inoperable non-small-cell lung cancer. *Int J Radiat Oncol Biol Phys* 2000;48:81–87.
27. Axford AT, Cotes JE, Deeley TJ, *et al.* Clinical improvement of patients with emphysema after radiotherapy. *Thorax* 1977; 32:35–39.
 28. Choi NC, Kanarek DJ, Kazemi H. Physiologic changes in pulmonary function after thoracic radiotherapy for patients with lung cancer and role of regional pulmonary function studies in predicting postradiotherapy pulmonary function before radiotherapy. *Cancer Treat Symp* 1985;2:119–130.
 29. Rietzel E, Chen GTY, Doppke K, *et al.* 4D computer tomography for treatment planning [Abstract]. *Int J Radiat Oncol Biol Phys* 2003;57(Suppl.):S232.
 30. Keall PJ, Joshi S, Tracton G, *et al.* 4-dimensional radiotherapy planning [Abstract]. *Int J Radiat Oncol Biol Phys* 2003;57(Suppl.):S233.
 31. Caldwell CB, Mah K, Skinner M, *et al.* Can PET provide the 3D extent of tumor motion for individualized internal target volumes? A phantom study of the limitations of CT and the promise of PET. *Int J Radiat Oncol Biol Phys* 2003;55:1381–1393.
 32. Choi NC, Fischman AJ, Niemierko A, *et al.* Dose-response relationship between probability of pathologic tumor control and glucose metabolic rate measured with FDG PET after preoperative chemo-radiotherapy in locally advanced non-small cell lung cancer. *Int J Rad Oncol Biol Phys* 2002;54: 1024–1035.